Available online at www.sciencedirect.com
ScienceDirect
Journal of Power Sources 159 (2006) 186–192
JOURNAL OF POWER SOURCES
www.elsevier.com/locate/jpowsour

Nanocrystalline TiO_2 (anatase) for Li-ion batteries

V. Subramanian [a], A. Karki [a], K.I. Gnanasekar [a], Fannie Posey Eddy [b], B. Rambabu [a,*]

[a] *Solid State Ionics and Surface Sciences laboratory, Department of Physics, Southern University and A & M College, Baton Rouge, LA 70813, USA*
[b] *National Center for Photovoltaics, National Renewable Energy Laboratory (NREL), 1617 Cole Blvd. Golden, CO 80401, USA*

Available online 30 June 2006

Abstract

Nanocrystalline TiO_2 (anatase) was synthesized successfully by the direct conversion of TiO_2-sol at 85 °C. The as-prepared TiO_2 at 85 °C were calcined at different temperatures and time in order to optimize the system with best electrochemical performance. The particle sizes of the synthesized materials were found to be in the range of 15–20 nm as revealed by the HR-TEM studies. Commercial TiO_2 anatase (micron size) was also studied for its Li-insertion and deinsertion properties in order to compare with the nanocrystalline TiO_2. The full cell studies were performed with $LiCoO_2$ cathode with the best performing nano-TiO_2 as anode. The specific capacity of the nanocrystalline TiO_2 synthesized at 500 °C/2 h in a half-cell configuration was 169 mAh g^{-1} while for the cell with $LiCoO_2$ cathode, it was 95 mAh g^{-1} in the 2 V region. The specific reversible capacity and the cycling performance of the synthesized nano-TiO_2 anode in full cell configuration across $LiCoO_2$ cathode are superior to that reported in the literature. Cyclic voltammetry measurements showed a larger peak separation for the micro-TiO_2 than the nano-TiO_2, clearly indicating the influence of nano-particle size on the electrochemical performance.

Keywords: TiO_2; Nanocrystalline; Insertion; Anatase; Anode; Lithium battery

1. Introduction

Titanium dioxide has been a well-known material for years because of its wide range of applications in solar cells, energy storage and environmental applications, such as photocatalysts for air purification, filters, etc. [1,2]. The reasons for TiO_2 being given more attention than other materials, such as ZnO, CdS, $ZrTiO_4$, etc., showing similar properties are better chemical stability, lower production cost and thin-film transparency [3–5]. The efficiency of the material in the above-mentioned applications mainly depends on the particle size and pore morphology of TiO_2.

In recent years, interest in the lithium insertion/deinsertion in nanocrystalline oxides has increased owing to the improved electrochemical properties. Tarascon and co-workers synthesized a variety of nano-phase transition metal oxides, such as CoO, MnO_2, Fe_2O_3, CuO, etc., and demonstrated excellent improvement in the electrochemical properties when used as anode materials in lithium batteries [6–8]. Dahn and co-workers have recently studied in detail the fundamentals behind the improved electrochemistry of nanocrystalline oxide anode materials [9].

Titanium dioxide exists in different polymorphic forms, such as rutile, anatase and brookite. Of the various polymorphs of TiO_2, both the rutile and brookite can accommodate only small amounts of lithium, while the anatase phase has different ratios of lithium insertion [10]. Recently, lithium insertion into TiO_2 with a ramsdellite phase has been reported [11]. Here, the lithium insertion coefficient was found to be 0.85 at room temperature. In the case of anatase TiO_2, there was an observed increase in the lithium insertion levels when the cycling was performed at 120 °C [12]. Synthesis of TiO_2 in nano-phase architecture has gained importance in recent years. The nature of the synthesized particles shows a strong dependence on the synthesis route adopted. Various methods, such as precipitation, sol–gel, emulsion, hydrothermal, etc., have been employed to synthesize the nano-particles of TiO_2 [13–16]. Lot of theoretical studies on the Li-intercalation in different forms of TiO_2 has been done using crystal orbital and Hartree–Fock calculations [17,18]. Lithium insertion into TiO_2 (anatase) was studied extensively using in situ X-ray diffraction, XPS and ^{7}Li NMR studies [19–21]. The in situ diffraction studies revealed that there was a completely reversible phase transformation from tetragonal anatase TiO_2 to orthorhombic anatase $Li_{0.5}TiO_2$ [19]. Li NMR studies proved that there was continuous flow of Li between lithium poor $Li_{0.01}TiO_2$ and lithium rich $Li_{0.06}TiO_2$ [21].

* Corresponding author. Tel.: +1 225 771 2493; fax: +1 225 771 2310.
E-mail address: rambabu@grant.phys.subr.edu (B. Rambabu).

0378-7753/$ – see front matter © 2006 Elsevier B.V. All rights reserved.
doi:10.1016/j.jpowsour.2006.04.027

Apart from nanocrystalline TiO_2, Li intercalation into single crystal phases has also been reported [22]. Preparation of mesoporous phase of TiO_2 is also considered to be equally important in the energy storage aspects, as the porosity plays an important role in the insertion–deinsertion reactions. Peng et al. reported mesoporous Sn-doped TiO_2 as lithium battery anodes with excellent reversibility [23]. However, the problem in the formation of mesoporous TiO_2 with stable pore walls is difficult unlike silica materials [24]. The main problem with TiO_2 is that it crystallizes easily during the calcination process destroying the mesoporous nature of the system. In the open literature, many reports are available for the electrochemical performance of TiO_2 as thin films [25–27]. However, only a few groups have reported the electrochemical properties of nanocrystalline phases. Also, probing the effects of calcination temperature and time on the structural and electrochemical properties will lead to a material that shows excellent electrochemical performance.

In this paper, we report the synthesis and electrochemical properties of nanocrystalline TiO_2 prepared by the direct conversion of the sol. The effect of calcination temperature and time on the structural and electrochemical properties have been studied using XRD, galvanostatic cycling, cyclic voltammetry (CV) studies.

2. Experimental

2.1. Synthesis

Titanium isopropoxide, 2-proponal were procured from Aldrich and used without any further purification. TiO_2 was synthesized according to the procedure, reported elsewhere [28]. In brief, titanium isopropoxide was diluted in 2-proponal. The resulting solution was hydrolyzed slowly by drop wise addition of water. The fine suspension of TiO_2-sol was gradually heated at 85 °C under constant stirring. The precipitate formed was collected and dried at 85 °C. Further calcination was done at different temperatures in order to improve the crystallinity.

The $LiCoO_2$ was synthesized by conventional solid-state method by mixing Li_2CO_3 and Co_3O_4 in a 1:1 mole ratio and firing the mixture at 800 °C for 30 h in air. The black powder after cooled to room temperature was ground and studied for its structural properties and phase purity.

2.2. Structural studies

The X-ray diffraction was done using *Siemens D5000* diffractometer in the 2θ range between 10° and 70°. HR-TEM measurements were made to investigate the particle size of the systems. The samples were dispersed in methanol and transferred to a *Holey Carbon grid* and the HRTEM and SAED measurements were obtained on a JEOL JEM2010 (200 kV) transmission electron microscope.

2.3. Electrochemical studies

The electrochemical performance of the TiO_2 (micro and nano) prepared at different temperatures were studied by assembling two-electrode HS-Test Cells (Hohsen Corp., Japan) with lithium metal as an anode in a 1 M $LiPF_6$ + EC + DMC (1:1 in volume) electrolyte. The electrode materials were prepared by mixing the active material with 10% PVdF binder and 10% conducting carbon black additive in NMP. The well-mixed slurry was coated on to a copper foil using doctor blade method. The coated foil was allowed to dry in an oven at 110 °C for 1 h and 30 m and then uniaxially pressed for better contact of the coated material and the copper current collector. Circular disc electrodes were punched from the foil and used as cathode for assembling the test cells. All manipulations were performed in a glove box filled (Vacuum Atmospheres, USA) with purified argon. The moisture content and oxygen level were less than 2 ppm inside the glove box. The assembled cells were discharged and charged galvanostatically at a constant current of 0.13 mA cm^{-2} between 2.5 and 1.0 V in a multi-channel battery tester (Arbin ABT 2043). Similar procedure was adopted to prepare the $LiCoO_2$ electrodes, instead the slurry was coated on to an aluminum foil and the cycling was performed between 1.0 and 2.5 V at a constant current density, 0.13 mA cm^{-2}.

Cyclic voltammetry was performed in an HS-Test cell in a two-electrode configuration. The cells were assembled inside an argon-filled glove box with lithium metal foil as counter and reference electrodes and the TiO_2 as a working electrode. The cyclic voltammetry experiment was performed using an EG&G Poten-

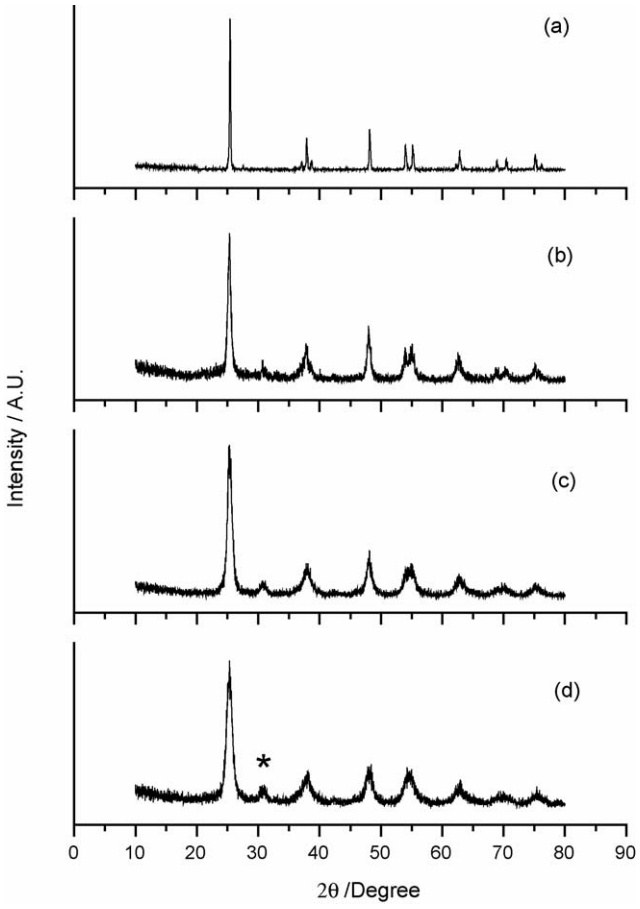

Fig. 1. X-ray diffraction patterns for anatase TiO_2 synthesized at different temperatures: (a) micro-TiO_2; (b) 500 °C/2 h; (c) 500 °C/4 h; (d) 600 °C/2 h (asterisk (*) indicates the brookite phase).

tiostat/Galvanostat (Model 273A) at a scan rate of 100 $\mu V\ s^{-1}$ between 2.5 and 1.0 V.

3. Results and discussions

3.1. X-ray diffraction studies

Fig. 1 shows the X-ray diffraction patterns of nano-TiO_2 calcined at different temperatures and the commercial TiO_2 (micro). The diffractograms show clearly the formation of phase pure TiO_2 in anatase phase. However, for the nano-TiO_2 synthesized in the lab, there is a trace amount of brookite phase coexisted with the anatase phase as indicated in the figure. There are many earlier reports available for the presence of small amount of brookite phase with the nano-TiO_2 [29]. The XRD profile even for the material calcined at 600 °C shows broad peaks revealing the nano-size of the particles. In the case of commercial TiO_2 (Aldrich), the XRD profile shows sharp peaks indicating the microstructure of the particles.

3.2. HRTEM and SAED analysis

The HRTEM pictures for the TiO_2 prepared at different temperatures are shown in Fig. 2. The average particle size for the TiO_2 calacined at 500 °C is 15–20 nm. Increasing the calcination temperature to 600 °C showed a little increase in the particle size as expected. This is mainly because TiO_2 has a general tendency to crystallize faster. The HRTEM results agree well with the XRD studies, where there has been a broad peak profile indicating the presence of nano-particles.

The SAED pattern for TiO_2 calcined at 500 °C is shown in Fig. 2(d). The diffraction rings 1–6 (from the center) have a lattice spacing of 3.5, 2.9, 2.4, 1.9, 1.7 and 1.5 Å. It is clear from the electron diffraction pattern that all the rings correspond to the anatase phase of TiO_2 except the diffraction ring 2, which is the characteristic reflection of brookite phase. This complements the XRD results on the presence of small amount of brookite phase along with the anatase phase.

3.3. Electrochemical studies

3.3.1. Charge–discharge studies

The charge–discharge curves for TiO_2 prepared at different temperatures are shown in Fig. 3. The charge–discharge studies were performed with TiO_2 as cathode and Li-metal anode in a 1 M $LiPF_6$:EC:DMC as electrolyte. As can be seen, there is a plateau in the 1.75 V region for all the TiO_2 studied. The nano-TiO_2 synthesized at different temperatures showed excel-

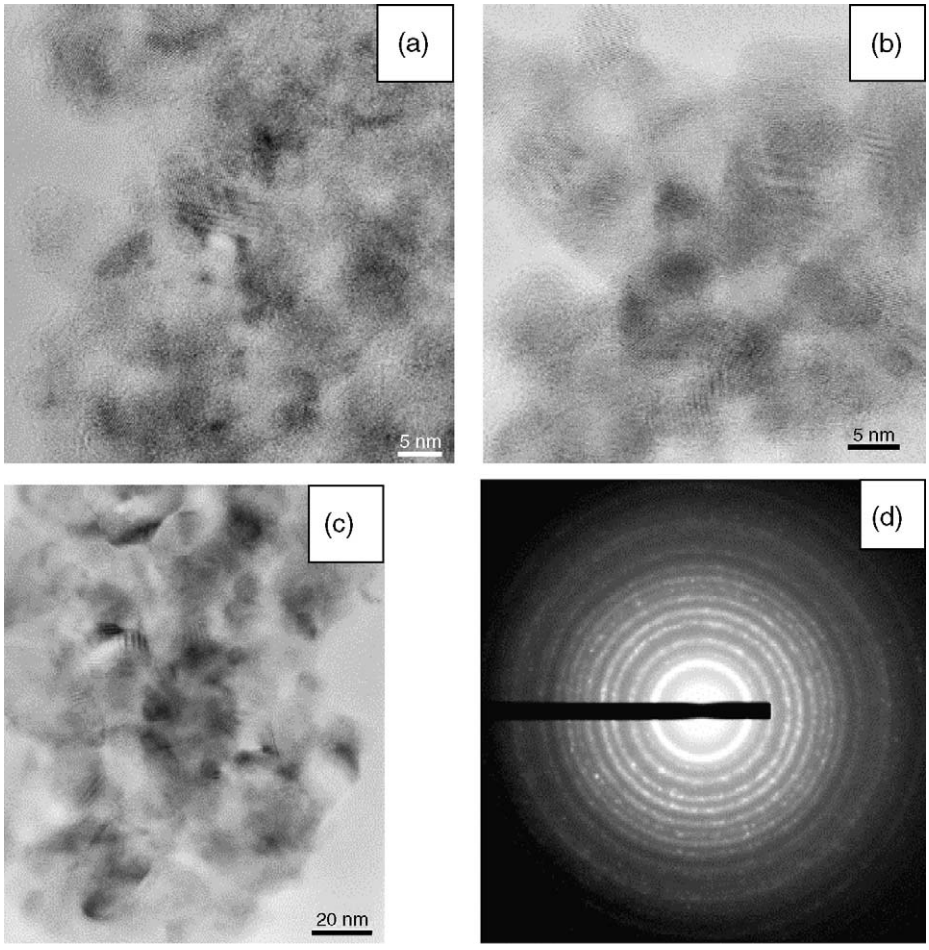

Fig. 2. HRTEM images of TiO_2 prepared at: (a) 500/2 h; (b) 500 °C/4 h; (c) 600 °C/2 h; (d) SAED patterns of TiO_2 prepared at 500 °C/2 h.

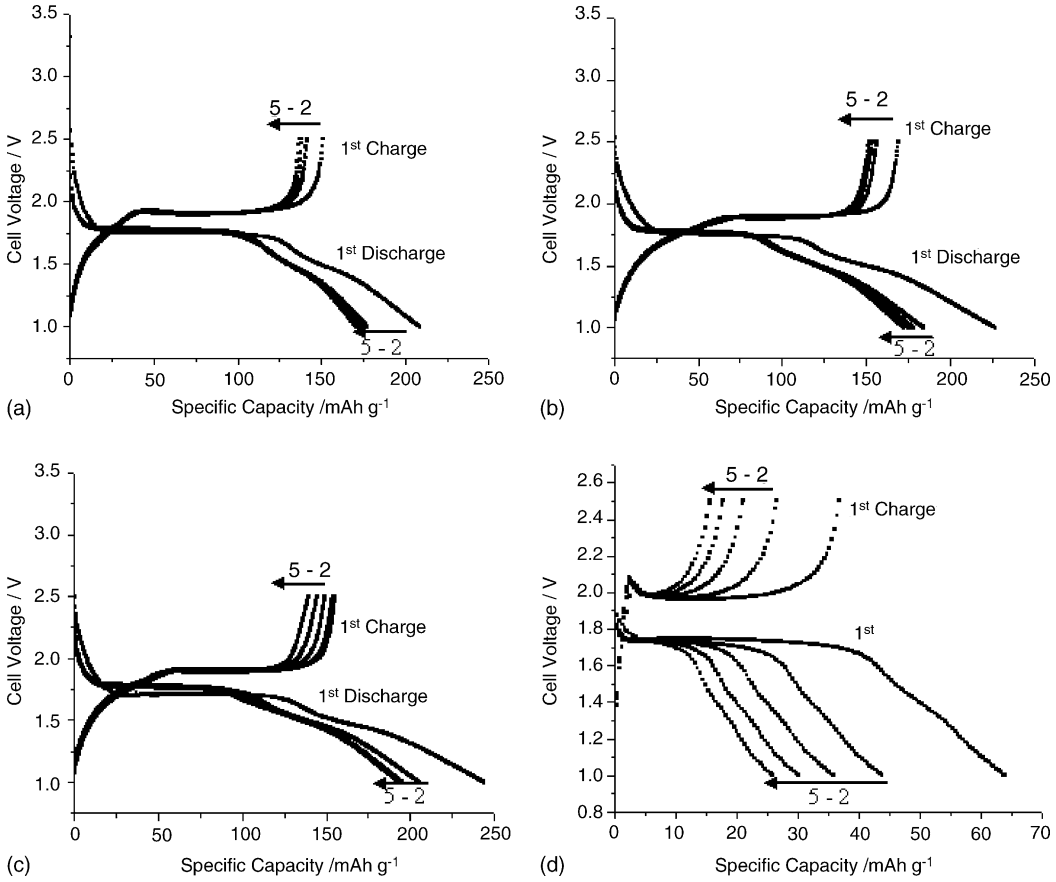

Fig. 3. Charge–discharge curves for TiO_2 prepared at different temperature: (a) 500 °C/2 h; (b) 500 °C/4 h; (c) 600 °C/2 h; (d) commercial (micro) TiO_2.

lent reversibility with a good cycling stability. The first cycle discharge capacity for the material prepared at 500 °C for 2 h was 230 mAh g^{-1} and the corresponding charging capacity is 169 mAh g^{-1}. There was a little decrease in the second cycle capacity with the discharge and charge capacity values of 180 and 156 mAh g^{-1}, respectively. In the case of the material prepared at 500 °C for 4 h, although the capacity value is higher than the material prepared at 500 °C/2 h, the fading is faster. The first and fifth cycle charge capacities are 155 and 139 mAh g^{-1}, respectively. The capacity showed a decrease when the calcination temperature was increased to 600 °C/2 h. The variation of specific charge capacity (reversible) with respect to cycle number for the different TiO_2 synthesized at temperature or calcined at different times is shown in Fig. 4. As can be seen, for all the nano-TiO_2 synthesized at different temperatures, the initial charge capacities were almost similar with the material prepared at 500 °C/2 h showing the highest. Also, this particular material shows a better cycling stability than the others do. It is clear that the material having the lower particle size and homogeneity will yield a better cycling performance. However, in the case of micro sized commercial TiO_2, there has been a faster fading and a poor electrochemical performance. The first cycle discharge capacity is 75 mAh g^{-1} and the corresponding reversible (charge) capacity is 37 mAh g^{-1}. Subsequently, after five cycles the charge capacity is 16 mAh g^{-1}. The present study clearly shows that nano-TiO_2 are better candidates as anode materials in Li-ion batteries than micro-TiO_2.

Although the theoretical capacity of anatase TiO_2 is 330 mAh g^{-1}, the practical achievable capacity is only half of

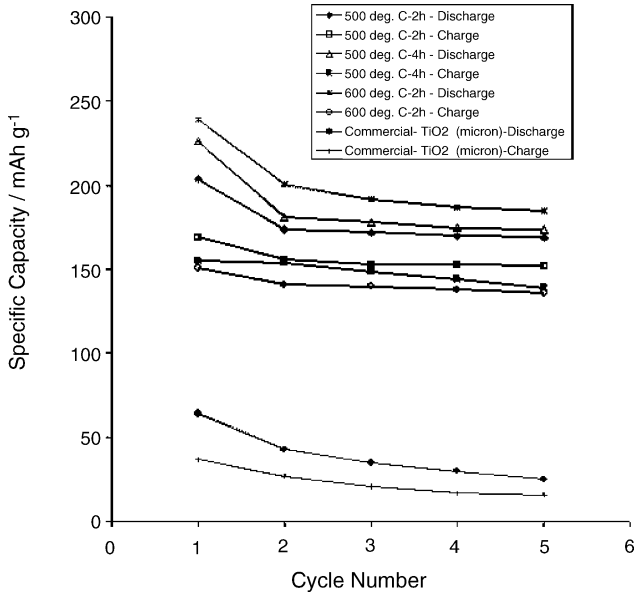

Fig. 4. Cycling performances of for TiO_2 prepared at different temperatures.

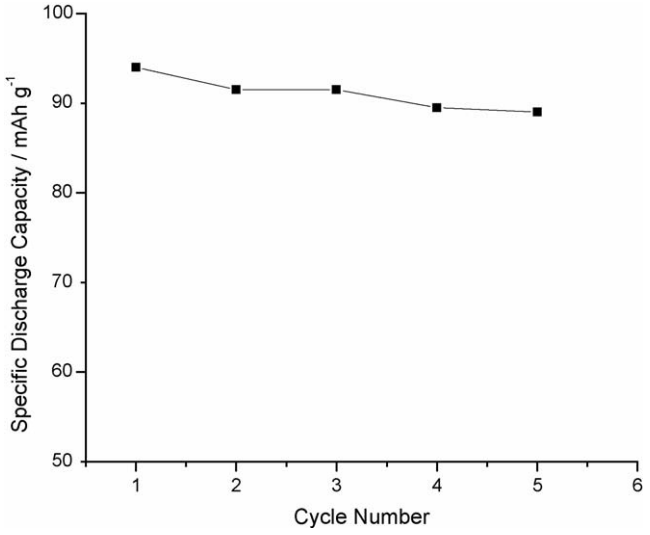

Fig. 5. Cycling performances of for $LiCoO_2/TiO_2$ full cell.

the available capacity. This is mainly because of the fact that, presence of Li greater than $x = 0.5$ in Li_xTiO_2 leads to strong Li–Li interaction in the lattice [30,31]. The main redox reaction responsible for the electrochemical activity is the conversion Ti^{4+}/Ti^{3+} during the discharge process and vice versa during the charge process.

In order to understand the battery performance in the 2 V region a full cell with $LiCoO_2$ as cathode and TiO_2 as anode was constructed and studied for its electrochemical properties. The system showed excellent cyclability with the first cycle reversible capacity of 95 mAh g^{-1} and the specific capacity after five cycles was 88 mAh g^{-1} as shown in Fig. 5.

The cell reaction can be written as:

$$TiO_2 + LiCoO_2 \Leftrightarrow Li_xTiO_2 + Li_{1-x}CoO_2$$

For a similar system with nanocrystalline anode and $LiCoO_2$ cathode, the reversible capacity was reported to be 55 mAh g^{-1} [32,33]. The possible reason for the higher capacity is the presence of more organized nano-structure of TiO_2 particles, which is derived from the merit of the synthesis technique adopted. Also, the current density in the present case is lower than that reported [32,33]. However, in the same work, the authors have reported that there is no greater than 10–15 mAh g^{-1} difference for the same system, when the current density was changed from 0.33 to 0.99 mA cm^{-2} [32,33]. So it is clear that the improved electrochemical properties for the present system with $LiCoO_2$ is mainly attributed to the more homogeneous nanoparticles. The present system with $LiCoO_2/TiO_2$ and 1 M $LiPF_6$ in EC:DMC electrolyte showed very good performance, contrary to that reported [32]. The authors have attributed the poor performance of the system to the lower conductivity of the electrolyte, 1 M $LiPF_6$ in EC:DMC. However, in the present study, there were no such poor performance for any of the TiO_2 half-cell or the $LiCoO_2/TiO_2$ full cell systems was observed. In order to understand the redox reactions taking place during the insertion–deinsertion of Li into TiO_2, cyclic voltammetry experiments were performed and the results are discussed in the next section.

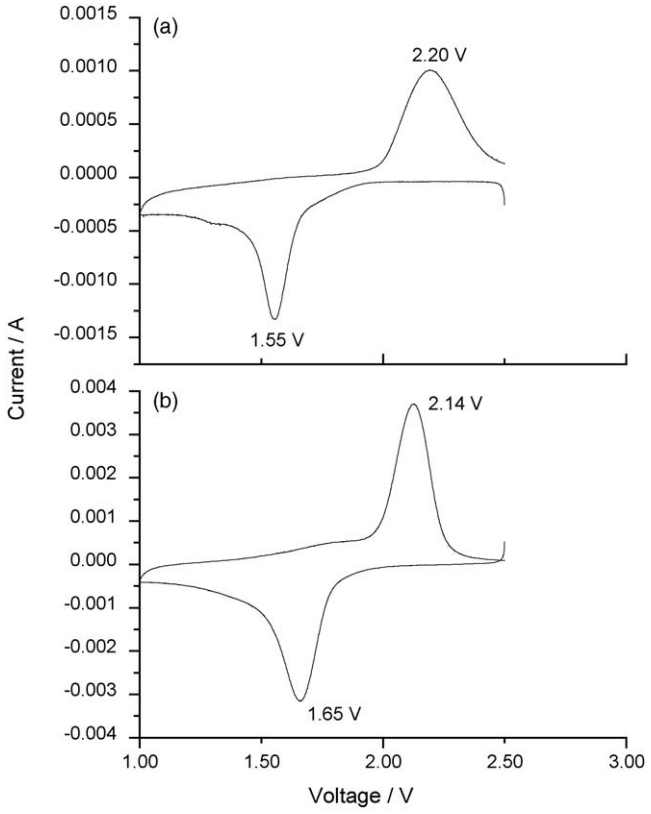

Fig. 6. Cyclic voltammograms of TiO_2 (a) micro-TiO_2 and (b) nano-TiO_2 (500 °C/2 h).

3.3.2. Cyclic voltammetry (CV) studies

The cyclic voltammograms recorded for nano-TiO_2 500 °C/2 h and commercial (micro) TiO_2 (Aldrich) are shown in Fig. 6. For the TiO_2 at 500 °C/2 h, the reduction of Ti^{4+} to Ti^{3+} takes place at 1.65 V and the corresponding deinsertion (oxidation) takes place at 2.14 V. In the case of commercial TiO_2 with micron particles, the profile remains the same as the nano-TiO_2 systems except the redox potentials and the associated current.

The overall cell reaction for the Li insertion/deinsertion reaction in TiO_2 can be written as:

$$TiO_2 + xLi^+ + xe^- \Leftrightarrow Li_xTiO_2$$

As explained in the previous section, the Li insertion was limited to a maximum x value of 0.5. The voltammetric anodic and cathodic charges were calculated by integrating the area of the respective regions of the CV curve. It has been proved by various analytical techniques that the transformation from TiO_2 anatase to $Li_{0.5}TiO_2$ anatase is a completely reversible reaction [19–21]. ^7Li NMR studies of TiO_2 with different levels of Li-insertion and de-insertion proved that when Li is inserted there is an observed two phase formation with one phase being Li rich while the other being Li poor phase and there is an observed high lithium flux between these phases [21].

Table 1
Voltammetric charge and peak potential values calculated from CV studies

System	Voltammetric charge (C g^{-1})		Peak potential separation (mV)
	Anodic	Cathodic	
Nano-TiO_2 500 °C/2 h	825	760	490
Micro-TiO_2 (Aldrich)	256	242	650

The voltammetric charge values and the peak separation for the systems studied are summarized in Table 1. As can be seen from the table, the cathodic charge is more than the anodic charge for all the TiO_2 systems with the commercial (micron) TiO_2 showing the lowest. This agrees well with that of the charge–discharge studies, supporting our earlier conclusion that nanocrystalline TiO_2 shows better performance as an anode material than the microcrystalline TiO_2.

Analysis of the CV curves with respect to the peak-peak potential separation in the anodic and cathodic region shows a highest value of ca. 0.65 V for the micro-TiO_2. In the case of nano-TiO_2 prepared at 500 °C/2 h, the separation was found to be 0.49 V. This agrees well with the earlier findings that, the material with smaller particle size has the smaller peak separation [34]. The main reason for the difference in the separation of the peak potentials is that the peak separation is determined by the overpotential required for the transformation of TiO_2 to Li_xTiO_2 [34]. The overpotential is usually larger for the material with smaller surface area (micro particles) than that with larger surface area (nano-particles) [34].

4. Conclusions

Nanocrystalline TiO_2 was successfully prepared by the direct conversion of TiO_2-sol at 85 °C in to fine nano-TiO_2. X-ray diffraction studies showed single-phase anatase with a small fraction of brookite. The average particle size for the particle prepared at 500 °C was 15 nm as evidenced by HRTEM studies. Nano TiO_2 showed excellent electrochemical properties both with respect to Li-metal and as anode material in a $LiCoO_2$ cathode system. Increase in the calcination temperature did not show any appreciable change in the particle size. The system prepared at 500 °C/2 h showed highest capacity in the present study with a reversible capacity of 170 mAh g^{-1}. The cycling performance was also found to be the best for this system with a cycling efficiency of 95% for five cycles. Increase in the calcination time and temperature although did not show any appreciable change in the capacity value, but the cycling performance showed dependence. Similar studies on microcrystalline TiO_2 yielded poor electrochemical properties for the system with a first cycle reversible capacity of 30 mAh g^{-1} while after five cycles it faded to 15 mAh g^{-1}. For a full cell, the system showed excellent 2 V activity with a reversible capacity of 90 mAh g^{-1}. This method of direct conversion of TiO_2-sol to nano-TiO_2 proves to be very efficient in terms of the electrochemical performance of the system.

Acknowledgments

The US-DOD-ARO is gratefully acknowledged for supporting this work (grant No. DAAD-19-01-1-0743). V.S. thanks the US-DOD-ARO for the senior research associate position. The authors also thank Dr. T. Prem Kumar, CECRI, Karaikudi, India, for helpful discussions.

References

[1] D. Bahnemann, D. Bockelmann, R. Goslich, Solar Energy Mater. 24 (1991) 564.
[2] K. Terabe, K. Kata, H. Miyazaki, A. Imai, J. Mater. Sci. 29 (1994) 1617.
[3] D.F. Ollis, E. Pellizzetti, N. Serpone, Environ. Sci. Technol. 25 (1991) 1523.
[4] J.A. Navio, G. Colvin, J.M. Herrman, J. Photochem. Photobiol. A: Chem. 108 (1997) 179.
[5] A.L. Linsebigler, G. Lu, J.T. Yates Jr., Chem. Rev. 95 (1995) 735.
[6] P. Poizot, S. Laruelle, S. Grugeon, L. Dupont, J.M. Tarascon, Nature 407 (2000) 496.
[7] F. Badway, I. Plitz, S. Gugeon, S. Laruelle, M. Dolle, A.S. Gozdz, J.M. Tarascon, Electrochem. Solid-State Lett. 5 (2002) A115.
[8] P. Poizot, S. Laruelle, S. Grugeon, L. Dupont, J.M. Tarascon, J. Power Sources 97–98 (2001) 235.
[9] M.N. Obrovac, R.A. Dunlap, R.J. Sanderson, J.R. Dahn, J. Electrochem. Soc. 48 (2001) A576.
[10] D.W. Murphy, R.J. Cava, S.M. Zahurak, A. Santoro, Solid State Ionics 9–10 (1983) 413.
[11] A. Kuhn, R. Amandi, F. Garcia-Alvarado, J. Power Sources 92 (2001) 221.
[12] T. Ohzuku, T. Kodama, T. Hirai, J. Power Sources 14 (1985) 419.
[13] D.S. Seo, H. Kim, H.C. Jung, J.K. Lee, J. Mater. Res. 18 (2003) 571.
[14] I.M. Arabatzis, P. Falaras, Nano Lett. 3 (2003) 249.
[15] S.Y. Chae, M.K. Park, S.K. Lee, T.Y. Kim, S.K. Kim, W.I. lee, Chem. Mater. 15 (2003) 3326.
[16] T.J. Trentler, T.E. Denler, J.F. Bertone, A. Agarwal, V.L. Colvin, J. Am. Chem. Soc. 121 (1999) 1613.
[17] M.V. Koudriachova, N.M. Harrison, S.W. de Leeuw, Solid State Ionics 152–153 (2002) 189.
[18] G. Nuspl, K. Yoshizawa, T. Yambe, J. Mater. Chem. 7 (1997) 2529.
[19] R. van de Krol, A. Goossens, E.A. Meulenkamp, J. Electrochem. Soc. 146 (1999) 3150.
[20] S. Sodergren, H. Siegbahn, H. Rensmo, H. Lingstrom, A. Hagfeldt, S. Lindquist, J. Phys. Chem. B 101 (1997) 3087.
[21] M. Wagemaker, A.P.M. Kentgens, F.M. Mulder, Nature 418 (2002) 397.
[22] L. Kavan, D. Fattakhova, P. Krtill, J. Electrochem. Soc. 146 (1999) 1375.
[23] Z. Peng, Z. Shi, M. Liu, Chem. Commun. 2125 (2000).
[24] Y. Yue, Z. Gao, Chem. Commun. (2000).
[25] H. Lindström, S. Södergen, A. Solbrand, H. Rensmo, J. Hjelm, A. Hagfeldt, S.E. Lindquist, J. Phys. Chem. B 101 (1997) 7717.
[26] H. Lindström, S. Södergen, A. Solbrand, H. Rensmo, J. Hjelm, A. Hagfeldt, S.E. Lindquist, J. Phys. Chem. B 101 (1997) 7710.
[27] A. Solbrand, H. Lindstrom, H. Rensmo, A. Hagfeldt, S.E. Lindquist, S. Södergen, J. Phys. Chem. B 101 (1997) 2514.
[28] K.I. Gnanasekar, V. Subramanian, J. Robinson, J.C. Jiang, F.E. Posey, B. Rambabu, J. Mater. Res. 17 (2002) 1507.
[29] Q. Xu, M.A. Anderson, J. Am. Ceram. Soc. 77 (1994) 1939.
[30] L. Kavan, K. Kratochvilova, M. Gratzel, J. Electroanal. Chem. 394 (1995) 93.

[31] L. Kavan, J. Rathousky, M. Gratzel, V. Shklover, A. Zukal, J. Phys. Chem. B 104 (2000) 12012.
[32] S.Y. Huang, L. Kavan, I. Exnar, M. Gratzel, J. Electrochem. Soc. 142 (1995) L142.
[33] I. Exnar, L. Kavan, S.Y. Huang, M. Gratzel, J. Power Sources 68 (1997) 720.
[34] P. Krtil, D. Fattakhova, L. Kavan, S. Burnside, M. Gratzel, Solid State Ionics 135 (2000) 101.